

A dynamically and kinetically consistent mechanism for H₂ adsorption/desorption from Si(100)-2×1

Michelle R. Radeke and Emily A. Carter*

*Department of Chemistry and Biochemistry, University of California Los Angeles, 405 Hilgard Avenue,
Los Angeles, California 90095-1569*

(Received 13 May 1996)

Curiously, H₂ desorption from Si(100)-2×1 follows approximately first-order kinetics rather than the expected second-order kinetics, arousing interest about the mechanism involved in the desorption process. We investigate the energetics and rate constants of three proposed mechanisms for H₂ desorption from Si(100)-2×1, namely, the prepairing mechanism, the isomerization mechanism, and the isolated dihydride mechanism, using complete active space self-consistent-field and multireference single- and double-excitation configuration-interaction calculations. We find the desorption barrier for the isolated dihydride mechanism to be 2.49 eV, the only barrier in excellent agreement with the experimentally determined barrier (~2.5 eV). The isolated dihydride mechanism also provides the only calculated desorption rate constant close to experimental values. Finally, we show that this mechanism is able to explain the experimentally observed apparent violation of detailed balance of H₂ adsorption/desorption on Si(100), as well as other experimentally observed dynamics. [S0163-1829(96)07939-8]

I. INTRODUCTION

Hydrogen atoms poison reactions with the Si(100)-2×1 surface by tying up the active surface sites—the dangling bonds—making the desorption of H₂ a possible rate-limiting step for many reactions occurring on this surface, e.g., Si epitaxy by SiH₄ and Si nitridation by NH₃. On Si(100)-2×1, H₂ begins to desorb at ~700 K and reaches its peak at ~800 K.^{1,2} Thus, in cases where lower-temperature film growth may provide desirable properties, alternative means for desorbing H₂ must be employed—techniques which should be aided by determining the mechanism by which H₂ desorption takes place.

The pathway for desorbing H₂ from Si(100)-2×1 has aroused curiosity because of its unexpected kinetic and dynamic behavior. In Sec. II we review experimental and theoretical work pertaining to the kinetic mechanism for desorption. Since mechanisms proposed for the kinetics must be consistent with experimental observations of the dynamics for this system, in Sec. III we discuss these experimental observations as well as current theoretical explanations. Our theoretical method is explained in Secs. IV and V. Results and discussion of our examination of possible pathways for adsorption/desorption are given in Sec. VI along with our proposal for a mechanism which would be compatible with all available kinetic and dynamic observations. In Sec. VII, we summarize our conclusions.

II. KINETICS OF H₂ ADSORPTION/DESORPTION

One might expect a process wherein two atoms recombine via a random mechanism to be second order in H coverage, as is the case for H₂ desorption from metal surfaces and from Si(111)-7×7.³ Instead, H₂ desorption from the monohydride phase of Si(100)-2×1 [$\Theta_{\text{H}} \leq 1$ (ML)] follows roughly first-order kinetics.²⁻⁶ This unexpected dependence on H-atom coverage has led to many interesting proposals for the

mechanism of H₂ desorption from Si(100)-2×1.

Sinniah *et al.* proposed a mechanism that attempted to explain this anomalous conduct. This mechanism envisions desorption via a delocalized H, and achieves first-order kinetics if the rate-limiting step is the transition of a chemisorbed H atom to a two-dimensional delocalized state which then is able to diffuse and quickly capture a second chemisorbed H atom.^{2,4} However, this proposal fails to explain why second-order kinetics are observed on Si(111)-7×7 for H₂ desorption, since by its nature this mechanism should be structure independent. Also, H-atom diffusion is unlikely to be delocalized on Si(100)-2×1,⁷⁻⁹ which has a highly corrugated potential-energy surface as a result of the reactivity of the localized dangling bonds. (The Si-H bond strength, i.e., the well depth near a dangling bond, is ~3.47–3.90 eV^{10,11}.) Additionally, because a delocalized H atom would react with the chemisorbed H atom over a wide range of impact parameters, one should expect the incipient H₂ molecules to exhibit excited internal state distributions. This leaves unexplained the internal state distribution measurements of Shane, Kolasinski, and Zare using resonance-enhanced multiphoton ionization (REMPI), which show that H₂ desorbs *rotationally cold* (compared to the surface temperature) though vibrationally excited.^{12,13}

A mechanism that would be unique to the Si(100)-2×1 surface is the “prepairing” mechanism, suggested by Wise *et al.*,³ which consists of one-step desorption of two H atoms on the same dimer. Theoretical calculations^{10,11,14} and experimental¹⁵ observations suggest that H atoms are “prepaired” on the same dimer due to the stabilizing influence of the π bond on unoccupied dimers. Using this assumption, i.e., that it is more favorable to form a monohydride than it is to uncouple another dimer π bond and form two singly-hydrogenated dimers, in a simple statistical-mechanical model, D’Evelyn, Yang, and Sutco¹⁴ and more recently Yang and D’Evelyn¹⁶ illustrated that such a system follows first-order desorption kinetics. The prepairing of H atoms is

physically evidenced by scanning tunneling microscopy (STM) data taken by Boland, which showed that upon heating, submonolayer coverages of H atoms will pair up on Si dimers.¹⁵ However, Sinniah *et al.* designed isotope experiments to test the preparing hypothesis, and found complete isotope mixing in the hydrogen desorbed, indicating no preference for H atoms to be prepared on a dimer prior to desorption.²

Theoretical calculations which attempt to verify the existence and plausibility of a preparing transition state (TS) have had mixed results. Jing and Whitten¹⁷ searched for the TS using Si_9H_{14} cluster calculations at the complete active space self-consistent-field (CASSCF) level and found a symmetric TS and an asymmetric TS centered over one of the dimer Si atoms (which we will refer to as the asymmetric side-centered TS) for direct desorption of H_2 from H atoms paired on the same dimer. However, they dismissed direct desorption as a plausible pathway for H_2 desorption, since the energy required to overcome the symmetric and asymmetric side-centered barriers [calculated at the limited configuration-interaction (CI) level to be 3.74 and 3.68 eV, respectively, including zero-point energy (zpe) corrections] is much higher than the experimentally determined values ($1.95 \pm 0.1 - 2.86 \pm 0.2$ eV).²⁻⁶ Nachtigall, Jordan, and Sosa also concluded that H_2 desorption could not occur through a symmetric preparing TS, based on their local-spin-density theory (DFT) Si_9H_{14} cluster calculations which determined an activation energy of 3.9 eV (not including zpe corrections) for this process.¹⁸ Wu, Ionova, and Carter, on the other hand, searched for a preparing TS at the Hartree-Fock self-consistent field level (HFSCF) and were unable to find a TS for direct H_2 desorption from the dimer, presumably because of the lower level of theory they used.¹⁹

Theoretical support for H_2 desorption via the preparing mechanism comes from several DFT calculations,²⁰⁻²⁴ which find an activation barrier within the range of experimental values. These calculations include several six-layer slab calculations using C_s symmetry.^{20,22,24} Li *et al.*²⁴ used the local-density approximation (LDA) with a 6-Ry cutoff, and found a symmetric (TS) with an activation barrier of 2.67 eV (not including zpe corrections). Using a 12-Ry cutoff and a combined LDA, generalized gradient approximation approach (LDA-GGA), in which electronic densities calculated using LDA are used as input for the nonlocal exchange-correlation term in the GGA, Vittadini and Selloni²² found an asymmetric side-centered TS with an energy barrier for desorption of 2.4 eV (not including zpe corrections). They also found a barrier to desorption of 2.7 eV for an interdimer TS, a mechanism first proposed by Wu, Ionova, and Carter.¹⁹ However, we argue, as did Wu, Ionova, and Carter, that such a mechanism would not follow first-order kinetics, since there is no driving force to “prepare” the H atoms on neighboring dimers. Using the same method as Vittadini and Selloni²² and a more robust basis set (30-Ry cutoff), Kratzer, Hammer, and Nørskov²⁰ found a barrier of 2.50 eV (including zpe corrections) for one-step desorption via an asymmetric side-centered TS. They also found a symmetric preparing TS which is 0.08 eV lower in energy than the asymmetric TS. In agreement with the slab calculation of Kratzer, Hammer, and Nørskov,²⁰ Pai and Doren²³ used a cluster model of the surface and found an asymmetric side-centered TS with

an activation energy of 2.8 eV (including zpe corrections), at the nonlocal BLYP-DFT level.

Nonetheless, recent calculations by Nachtigall *et al.*²⁵ suggest that the agreement of DFT with experiment may be fortuitous, and therefore misleading about the mechanism. After all, since the true surface mechanism is unknown, matching barriers is only suggestive of, not unequivocal support for, a given mechanism. Nachtigall *et al.* showed that using better exchange-correlation functionals in DFT calculations, for instance the BLYP functional and more preferably the Becke3LYP functional, qualitatively changes the predictions made by DFT. Indeed their DFT calculations show that inferior DFT functionals significantly *underestimate* the known activation energies for H_2 elimination from SiH_4 and Si_2H_6 , as well as for other related gas-phase reactions with silanes. The method of calculation which Nachtigall *et al.* found to be closest to experiment in these cases is the extrapolated quadratic configuration interaction with single, double (and triple) excitations [E-QCISD(T)] method. Using E-QCISD(T) as an approximation of experimental values, they determined that less accurate DFT functionals also underestimate the activation energies for H_2 desorption from a Si_2H_6 cluster model for desorption from monohydride $\text{Si}(100)\text{-}2 \times 1$. In fact, using the Becke3LYP functional and the larger Si_9H_{14} cluster model, Nachtigall, Jordan, and Sosa¹⁸ obtained a barrier for the asymmetric side-centered TS of 3.2 eV, significantly higher than the slab or cluster calculations done using the inferior DFT functionals, and too high to explain experimental results.¹⁸ Given the apparent controversy between the DFT and *ab initio* CI predictions, we have undertaken more sophisticated MRSDCI (multireference single and double excitation configuration interaction) calculations than used previously to reexamine this pathway, as discussed below.

III. DYNAMICS OF H_2 ADSORPTION/DESORPTION

Any mechanism proposed to explain the H_2 desorption kinetics from $\text{Si}(100)\text{-}2 \times 1$ must also be consistent with experimental observations pertaining to the dynamics of the adsorption/desorption process. The most enigmatic experimental observation is the very low sticking probability (S_0) that H_2 has on bare Si surfaces ($\sim 10^{-6}$ at 800 K),^{26,27} suggesting that an extremely large barrier for the adsorption process exists. From traditional models of dynamics (i.e., detailed balance arguments), one assumes that adsorption and desorption happen through the same pathway. Hence, if H_2 desorbs via a pathway with a substantial adsorption barrier, then there should be an excess of energy in the desorbing molecule, as evidence that the desorbing H_2 came down off of a large adsorption barrier. However, REMPI measurements of internal state distributions by Kolasinski, Shane, and Zare¹² combined with time-of-flight measurements by Kolasinski *et al.*^{28,29} show that desorbing H_2 molecules do not possess much more energy than that provided by the zpe of H_2 and the bare surface. Thus experimentalists have found no evidence that H_2 surmounts an extremely large barrier in the adsorption process, and this apparent violation of microscopic reversibility presents a puzzle. Kolasinski and co-workers^{12,13,28,29} suggested that the large apparent adsorption barrier could be due to orientational restrictions to which

impinging H_2 molecules would be unable to conform. They proposed that the adsorbate has a relatively infinite amount of time to assume the orientation required by the desorption pathway, while impinging H_2 molecules have no time at all—thus they attributed the apparent lack of detailed balance to a time-scale difference between the adsorption and desorption processes.

REMPI measurements of H_2 internal state distributions made by Shane, Kolasinski, and Zare^{12,13} are similar for monohydride and dihydride Si(100), as well as for Si(111)-7×7, indicating that desorption occurs through a common intermediate on all three surfaces. Nachtigall, Jordan, and Janda¹⁰ and Shane, Kolasinski, and Zare^{12,13} proposed that desorption might occur from an isolated dihydride formed by a Si dimer monohydride [$H-Si-Si-H_{(a)}$] undergoing isomerization to a bare Si plus a dihydride [$Si_{(a)}+SiH_{2(a)}$]. The monohydride-dihydride isomerization mechanism would produce $SiH_{2(a)}$ on monohydride Si(100), and since this species would also be available on dihydride Si(100) and potentially on Si(111)-7×7, these surfaces would all share a common precursor. Wu, Ionova, and Carter¹⁹ searched the TS region at the HFSCF level using C_s symmetry, and showed the presence of a two-step pathway which consists of monohydride to dihydride isomerization followed by desorption from the dihydride. Using CI methods, they calculated the barrier to this process to be 4.09 eV, much too high to explain the experimental results. However, they noticed that it is the isomerization step which makes the energy barrier too high—the barrier to desorption from the bare Si plus dihydride is within the range of experimental values. Thus they proposed an alternate path to desorption—desorption from isolated dihydrides, which would most likely be formed transiently at defect sites.

Currently, several mechanisms strive to explain the apparent violation of detailed balance for the reaction of H_2 with Si(100)-2×1. One possibility is that while $SiH_{2(a)}$ might be relatively easy to form at certain defect sites, if the concentration of these defects is small this would lead to a tiny S_0 .^{18,19,31} Kolasinski *et al.*²⁸ pointed out that this explanation would require the concentration of defects to be as negligible as the S_0 ($<10^{-6}$). Furthermore, this mechanism would require similarly small numbers of defect sites on the Si(111)-7×7 surface as on the Si(100)-2×1 surface, since the S_0 on the Si(111)-7×7 surface is also extremely small. Jing, Lucovsky, and Whitten answered the first criticism, regarding the required scarcity of defects on the Si(100)-2×1 surface, by noting that the number of active sites for desorption is not necessarily equal to the defect concentration, since it is an activated process to form the dihydride from which desorption will occur.³¹ However, this does not explain the low S_0 on the Si(111)-7×7 surface which has many single-atom sites and is very topologically different from the Si(100)-2×1 surface. It is possible to rationalize the presence of many more isolated Si atoms on the Si(111)-7×7 surface versus the Si(100)-2×1 surface, since single Si atoms on the Si(111)-7×7 surface would be bonded to three subsurface Si atoms and thus be monovalent and unready sites for H_2 adsorption. Nonetheless, this scenario still depends on similar concentrations of defects leading to $SiH_{2(a)}$ on both Si surfaces.

An alternative explanation to this puzzle is offered by

Brenig, Gross, and Russ,³² who modeled the effect of local lattice relaxation in H_2 adsorption/desorption, and proposed that desorbing H_2 molecules do come off of a large barrier to adsorption, but that the excess energy is released into the Si lattice coordinates. In their model, incident H_2 molecules experience a large adsorption barrier, which can be modulated by phonons. Brenig, Gross, and Russ predicted that sticking is assisted by phonons, and thus would increase with increasing surface temperature, in agreement with recent experimental observations.^{26,28,29}

Kratzer, Hammer, and Nørskov,²⁰ and, independently, Pehlke and Scheffler²¹ suggested that the preparing mechanism could explain the temperature dependence of the sticking probability. Their slab DFT calculations found that the barrier to adsorption of H_2 on the Si(100)-2×1 surface via the preparing mechanism is highest when the Si dimer is highly buckled, which their calculations determined to be the minimum-energy configuration for the Si(100)-2×1 surface. When the buckling of the dimer is more moderate, however, they predicted that the adsorption barrier becomes much smaller. For instance, Kratzer, Hammer, and Nørskov calculated that H_2 adsorbing onto a dimer would see a 0.67-eV static barrier, which can be reduced to 0.42 eV when the degree of Si dimer buckling is optimized. They proposed that at low temperatures the sticking probability would be small due to the 0.67-eV barrier, while at higher temperatures the sticking probability would increase, as there would be more thermal energy available for the dimer to contort, thus explaining the experimentally observed^{26,28} temperature dependence of the sticking probability. However, molecular-dynamics simulations³³ suggest that the dimers on the Si(100)-2×1 surface are actually rapidly converting from buckled to unbuckled configurations, and that the degree of dimer buckling increases with increasing temperature. Since the dimer buckling is related to surface phonons, and since vibrational amplitudes increase with temperature, one should expect buckling to increase with temperature, regardless of the nature of the actual minimum-energy configuration. Thus, the more moderate dimer buckling which Kratzer, Hammer, and Nørskov²⁰ and Pehlke and Scheffler²¹ predict to be the most favorable configuration for adsorption may be more likely to occur at lower temperatures, not higher ones.

The large “static” adsorption barrier for this “buckled preparing” mechanism is consistent with the experimentally observed low sticking probability, but not with the low adsorption barrier (77 ± 80 meV) Kolasinski *et al.*²⁹ predicted based on H_2 desorption experiments. Even the buckling-modulated barrier of 0.42 eV would require that a substantial amount of energy be dumped into the surface coordinates during H_2 desorption. Moreover, since this mechanism involves Si dimers, it does not explain a similar enhancement of sticking probability with increasing surface temperature observed for the dimer-free Si(111)-7×7 surface,³⁴ nor does not provide for an intermediate to desorption that could be common on both the Si(111)-7×7 and Si(100)-2×1 surfaces.

IV. THEORETICAL APPROACH

We investigate the TS region for the desorption of H_2 from Si(100)-2×1 in order to access adsorption/desorption through the preparing, isomerization, and isolated dihydride

mechanisms. We find all of the TS's reported above for these mechanisms plus two additional TS's that have not been previously reported. Additionally, we also look at desorption from the dihydride Si(100)-1 \times 1 surface ($\Theta_{\text{H}}=2.0$ ML). Our investigation of these pathways uses a higher level of calculation than was possible previously. Modern workstations and parallel computing allow us to perform saddle-point searches starting from product and reactant at the CASSCF level, using large clusters (21–26 atoms representing 4–5 layers of Si). Calculating the TS at the CASSCF level is important, since it allows full electron correlation within the space involved in the reaction. A recent analysis by Jing and Whitten¹⁷ comparing the HFSCF and CASSCF methods illustrated that, while HFSCF does well at finding asymmetric TS's, CASSCF level calculations are necessary to find symmetric TS's, due to symmetry breaking that often occurs in HFSCF calculations. Furthermore, we determine whether each of the TS's is indeed a true TS (i.e., a saddle point of rank one). As it is preferable to compare rate constants for H₂ desorption via the many proposed mechanisms, since these are the actual measured quantities rather than the activation energies, we provide the only estimates available of rate constants for desorption through each of these pathways.

V. DETAILS OF THE CALCULATIONS

A. Modeling the surface

We use two types of clusters for these calculations, which consist of Si atoms terminated by ‘‘siligens’’ ($\bar{\text{H}}\text{'s}$), H atoms whose basis set has been modified to reproduce the electronegativity of Si, so that there is no charge drawn off the cluster.^{35,36} The monohydride is modeled by the Si₉ $\bar{\text{H}}_{12}$ H₂ cluster [Fig. 1(a)] which contains two surface Si atoms, four second-layer Si atoms, two third-layer Si atoms, and one fourth-layer Si atom, plus two adsorbate H atoms. The isolated dihydride is represented by the Si₁₀ $\bar{\text{H}}_{14}$ H₂ cluster [Fig. 1(b)] which includes one surface Si atom, two second-layer Si atoms, four third-layer Si atoms, two fourth-layer Si atoms and one fifth-layer Si atom, plus two adsorbate H atoms. In all of the calculations, the $\bar{\text{H}}\text{'s}$ are fixed in bulk Si, tetrahedral positions with an optimized Si-H bond length of 1.729 Å,³⁶ so as not to distort the cluster during subsequent geometry minimizations. This allows the cluster to better represent a bulk lattice geometry.

The $\bar{\text{H}}\text{'s}$ that terminate the cluster are represented by a three Gaussian minimum basis set.³⁶ For each of the Si atoms, an effective-core potential (ecp) is used, so that only the valence electrons are described by a double ζ basis set.³⁷ We add a 3d polarization function ($\zeta^d=0.3247$) to the surface silicon(s). The adsorbate H atoms each are represented by the Dunning triple- ζ contraction³⁸ of the Huzinaga 6s Gaussian basis set³⁹ with the addition of one 2p polarization function ($\zeta^p=0.6$).

We use a four-orbital, four-electron CAS (20-spin eigenfunctions) defined as the two Si-H bonds and their antibonds for the Si₁₀ $\bar{\text{H}}_{14}$ H₂ cluster and a six-orbital, six-electron CAS (175 spin eigenfunctions) for the Si₉ $\bar{\text{H}}_{12}$ H₂ cluster, where the two additional orbitals represent the Si dimer bond and antibond. To represent the dihydride phase ($\Theta_{\text{H}}=2$ ML), we use a Si₉ $\bar{\text{H}}_{12}$ H₄ cluster and an eight-orbital, eight-electron CAS (1764 spin eigenfunctions) which includes the four Si-H

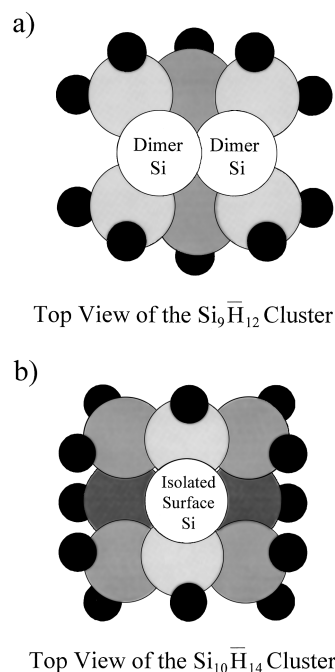


FIG. 1. (a) The Si₉ $\bar{\text{H}}_{12}$ and (b) Si₁₀ $\bar{\text{H}}_{14}$ clusters are used to model a surface Si dimer and an isolated Si, respectively. The black spheres symbolize the embedding siligens ($\bar{\text{H}}\text{'s}$). (a) The Si₉ $\bar{\text{H}}_{12}$ cluster is comprised of two surface Si atoms representing the surface dimer (white spheres), four second-layer Si atoms (light gray spheres), two third-layer Si atoms (medium gray spheres), and one fourth-layer Si atom (hidden). (b) The Si₁₀ $\bar{\text{H}}_{14}$ cluster consists of one surface Si atom representing an isolated surface Si (white sphere), two second-layer Si atoms (light gray spheres), four third-layer Si atoms (medium gray spheres), two fourth-layer Si atoms (dark gray spheres), and one fifth-layer Si atom (hidden).

bonds and their antibonds. To keep the CAS reference consistent for desorption products (H_{2(g)}+surface), we use a ‘‘super system,’’ wherein the H₂ molecule is placed at an effectively infinite (noninteracting) distance from the cluster representing the surface (~ 7 Å).

The various adsorbed and desorbed structures are optimized using a quasi-Newton method⁴⁰ at the CASSCF level using C_s symmetry, and TS searches are also done at this level of theory using C_s symmetry. This provides for 15 and 17 degrees of freedom in the Si₉ $\bar{\text{H}}_{12}$ and the Si₁₀ $\bar{\text{H}}_{14}$ clusters, respectively. There are two additional degrees of freedom for each H adsorbate.

For all of our TS searches we use the Ridge method,⁴¹ which allows us to start the searches knowing only the structures of the product and reactant. The Ridge method was recently modified to include the direct inversion in the iterative subspace algorithm, which can speed up TS searches considerably.⁴² Once a TS is obtained, we verify that it is a TS of rank 1 (i.e., a saddle point) by computing the Hessian (energy second-derivative matrix) to determine that only one negative eigenvalue is present. We also walk down on each side of the ridge containing the saddle point to ascertain the product and reactant connected by the TS are those for the desired reaction. The Hessians are computed numerically from finite differences of analytical gradients using a displacement from the optimal geometry of 0.01 bohr, at the same CASSCF level at which the TS was searched. Two-

point sampling, in which equal displacements in the positive and negative directions are made so that two times $3N$ displacements were made (where N is the number of unique atoms), allowed for improved accuracy in the Hessian calculations. We note that it would be preferable to evaluate the Hessians analytically, but this technique is not currently available for CASSCF wave functions using ecp's. All CASSCF energy calculations and Hessian evaluations were performed using the program HONDO.⁴³

In order to determine the activation energies and the endothermicity of H_2 desorption to better accuracy, we calculate the energies of the CASSCF-optimized products, reactants and TS structures at the MRSDCI level.⁴⁴ We use the CAS reference for the CI, allowing single and double excitations from all the active orbitals to all virtual orbitals. This leads to 29 700 spin eigenfunctions for the $Si_9\bar{H}_{12}H_2$ cluster, 363 475 spin eigenfunctions for the $Si_{10}\bar{H}_{14}H_2$ cluster, and 5 950 980 spin eigenfunctions for the dihydride $Si_9H_{12}H_4$ cluster. The barrier heights and endothermicities are corrected by the zpe's which we obtain from the vibrational frequencies determined by diagonalization of the corresponding Hessian matrices.

B. Estimation of error

To estimate the error introduced by ecp's, a finite basis set, and the CASSCF/MRSDCI method for obtaining TS geometries and energetics, we used these same methods (described above in Sec. V A) to obtain endothermicities and activation energies for analogous gas-phase reactions (H_2 elimination from small gas phase silanes), where both the energetics and mechanism are well characterized and therefore serve as a calibration of our approach. H_2 elimination from silane (SiH_4) most closely resembles desorption from the $Si_{10}\bar{H}_{14}H_2$ cluster; thus we used this system to assess the error in our energetics for the isolated dihydride mechanism. On the other hand, the prepairing mechanism is better approximated by 1,2 elimination of H_2 from disilane (Si_2H_6), since this is also a four-center, four-electron process. In Secs. VI A and VI D, the strong similarity between the structures of the H_2 desorption TS's and their analogous gas phase TS's becomes evident, lending credibility to our estimations of error.

Table I compares the energetics we calculate for two different gas-phase silane reactions with values determined by other theoretical calculations and experiment.⁴⁵ Comparison of our value to the experimental values^{46,47} shows that we underestimate the reaction energy (E_{rxn}) by ~ 0.1 – 0.2 eV and overestimate $E_{a,forward}$ by the same amount. Since the activation energy for addition of silylene (SiH_2) to H_2 ($E_{a,reverse}$) is just $E_{a,forward} - E_{rxn}$, by combining our errors for $E_{a,forward}$ and E_{rxn} we find that we could be overestimating the activation energy for the addition process by ~ 0.2 – 0.4 eV or as much as 0.5 eV if we compare to Jasinski's estimate for this value.⁴⁸ Thus, we estimate our errors in ΔE_{rxn} and E_a for H_2 desorption from the dihydride state to be ≤ 0.2 eV too low and too high, respectively, and that E_a for H_2 adsorption into the dihydride state could be too high by as much as 0.2 – 0.5 eV. Experimental error could account for some of the discrepancy between our results for gas-

TABLE I. Comparison of calculated and experimental values of reaction and activation energies for two silane H_2 elimination and addition reactions. (All theoretical energies reported in this table include zpe corrections. The asterisk means not available.)

	E_{rxn} (eV)	$E_{a,forward}$ (eV)	$E_{a,reverse}$ (eV)
$SiH_4 \rightleftharpoons SiH_2 + H_2$			
MRSDCI (this work)	2.19	2.68	0.49
E-QCISD(T) ^a	2.35	2.48	0.13
MP4 ^b	2.39	2.47	0.08
experiment	2.40 ^c	2.42 ^c	<0.1 ^d
		2.25 ± 0.30 ^e	
$Si_2H_6 \rightleftharpoons Si_2H_4 + H_2$			
1,2 elimination			
MRSDCI (this work)	2.07	3.76	1.69
E-QCISD(T) ^a	2.03	3.68	1.65
MP4 ^f	2.04	3.73	1.69
experiment	1.95 ^g	*	*

^aFrom Ref. 25.

^bFrom Ref. 58.

^cFrom Ref. 46.

^dFrom Ref. 48. This value is an estimate based on other experimental values.

^eFrom Ref. 47.

^fFrom Ref. 56.

^gFrom Ref. 49.

phase silane energetics and experimental values, especially in regards to activation energies for these reactions which are not measured directly.

For H_2 elimination from disilane, we find a value for $E_{rxn} \sim 0.1$ eV higher than the experimental value (see Table I).⁴⁹ Since H_2 elimination from disilane is known to occur through a 1,1- rather than 1,2-elimination pathway, we must use the 1,2- H_2 -elimination activation barriers obtained by theoretical methods^{25,56} shown to be in good agreement (within 0.1 eV) with experimentally determined energetics for other silane gas phase reactions. Table I shows that we potentially overestimate $E_{a,forward}$ by <0.1 eV, and underestimate $E_{a,reverse}$ by ~ 0.04 – 0.1 eV. Thus, for the prepairing mechanism, these calibrations suggest that our activation energies for desorption and adsorption of H_2 will be too high and too low, respectively, by 0.1 eV.

As a check of our cluster approximation as a model of the real surface, we note that the CASSCF vibrational frequencies we calculate for the monohydride phase of $Si(100)$ - 2×1 (using the $Si_9\bar{H}_{12}H_2$ cluster) are 2144.1 and 2151.5 cm^{-1} for the Si-H stretches, compared to experimental values of 2087.5 and 2098.8 cm^{-1} .⁶ For the SiH_2 species (represented by the $Si_{10}\bar{H}_{14}H_2$ cluster) we obtain frequencies of 2142.1 cm^{-1} for the symmetric stretch, 2159.9 cm^{-1} for the asymmetric stretch, and 889.5 cm^{-1} for the scissors mode, compared to experimental values for these of 2091.3, 2103.8, and 910 cm^{-1} (for the symmetric, asymmetric and scissors modes, respectively).⁶ Our calculated harmonic frequencies are in quite good agreement with the experimental values; thus we expect the clusters used in this study to be reasonable models for adsorbates on the $Si(100)$ - 2×1 surface. We also note that the conformity of the barriers calculated for H_2

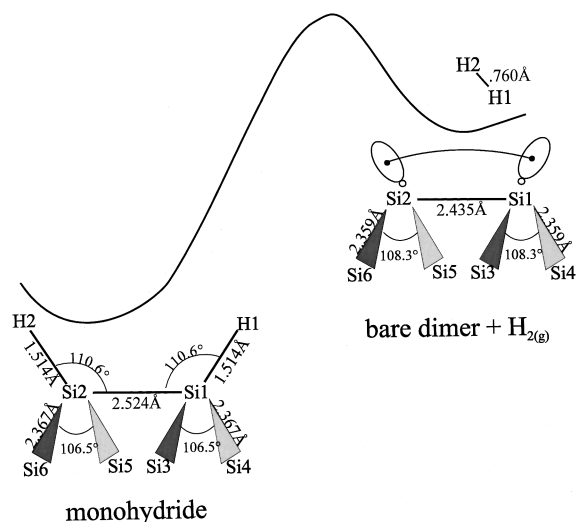


FIG. 2. The direct H_2 desorption pathway from a monohydride is illustrated, along with the geometries of the reactant and products.

desorption from $Si(100)-2\times 1$ via DFT slab and cluster models, mentioned previously, indicates that a finite cluster models this surface well.

C. Calculating rate constants

We calculate rate constants for each mechanism for which we are able to find a TS, using simple transition state theory (STST). In STST, the rate constant, k is given as the Arrhenius expression $k = A e^{(-E_a/k_B T)}$, where A is the preexponential factor, E_a is the activation energy for the reaction, k_B is the Boltzmann constant, and T is the system temperature. Since we already have determined the activation energy to be the difference between the MRSDCI total energies at the TS and of the reactant at its equilibrium structure, we only need the preexponential in order to estimate the rate constant. Within the harmonic potential approximation, we can write the preexponential as $A = (\prod^{3N-6} \nu_{\min} / \prod^{3N-7} \nu_{\text{sad}})$, which is the product of the nonzero vibrational frequencies at the minimum (the reactant) divided by the product of the real, nonzero vibrational frequencies at the TS.⁵⁰ (Recall that a true TS possesses only one imaginary frequency corresponding to the normal mode involved in converting from reactant to product.) We calculate the vibrational frequencies by diagonalizing the CASSCF Hessian matrix, and use this information in order to make an estimate of the preexponential, and thus an estimate of the order of magnitude of the rate constant for a given mechanism.

VI. RESULTS AND DISCUSSION

A. Preparing mechanism

Using the $Si_9\bar{H}_{12}H_2$ cluster, we searched the region between the products and reactants depicted in Fig. 2 for a TS for direct desorption. Our calculations yield an endothermicity for desorption via this route of 2.90 eV (including zpe corrections). Given the calibration in Sec. V B, we estimate the true endothermicity to be 2.8 eV. We found the symmetric and asymmetric side-centered TS's reported

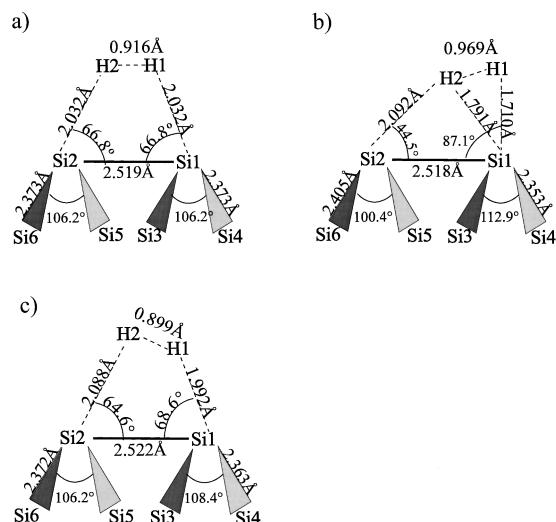


FIG. 3. Geometries of the three TS's for the preparing mechanism: (a) the symmetric TS, (b) the asymmetric side-centered TS, and (c) the asymmetric dimer-centered TS.

beforehand,^{17,18,20,22,23,24} and also an asymmetric TS centered over the dimer, which had not been determined previously.

The geometry we find for the symmetric TS corresponding to the preparing mechanism is given in Fig. 3(a); it is the only TS searched for using C_{2v} symmetry. Our prediction for this barrier is 3.55 eV (including zpe corrections) compared to the value of 3.74 eV (including zpe corrections) reported by Jing and Whitten,¹⁷ and 3.9 eV (no zpe corrections included) calculated by Nachtigall, Jordan, and Sosa.¹⁸ (Note that including zpe corrections in the activation energy calculated by Nachtigall, Jordan, and Sosa would lower their barrier.) We also note that the geometries of the TS's found by us and by Jing and Whitten are very close (a geometry from Nachtigall, Jordan, and Sosa is not available for comparison). In the TS structure we have found, the H-H bond is 0.92 Å, the Si-H bonds are 2.03 Å, and the Si-Si dimer bond is 2.52 Å compared to $R(\text{H-H})=0.93$ Å, $R(\text{Si-H})=2.03$ Å, and $R(\text{Si-Si})=2.41$ Å determined by Jing and Whitten. Our geometry for the symmetric TS, as well as that of Jing and Whitten, is also very close to the geometries determined by Li *et al.*²⁴ [$R(\text{Si-H})\sim 2.12$ Å and $R(\text{Si-Si})=2.44$ Å] and Kratzer, Hammer, and Nørskov²⁰ [$R(\text{H-H})=0.90$ Å, $R(\text{Si-H})=2.08$ Å, and $R(\text{Si-Si})=2.42$ Å]. Examinations of the vibrational frequencies of the symmetric TS made by both Kratzer, Hammer, and Nørskov *et al.*, and us, find that this TS is a rank-1 saddle point. However, Nachtigall, Jordan, and Sosa calculated HFSCF frequencies and found two imaginary normal modes, indicating a saddle point of rank 2. As noted earlier, HFSCF level calculations are inadequate descriptions of symmetric structures. Also, the TS found by Nachtigall, Jordan, and Sosa on the DFT potential-energy surface is not necessarily a TS on the HFSCF potential-energy surface.

For the asymmetric side-centered TS we find an activation energy of 3.68 eV (including zpe corrections) and a geometry [see Fig. 3(b)] of $R(\text{H1-H2})=0.97$ Å, $R(\text{Si1-H1})=1.71$ Å, $R(\text{Si1-H2})=1.79$ Å, $R(\text{Si2-H2})=2.09$ Å, and $R(\text{Si1-Si2})=2.52$ Å. Table II illustrates that six different groups using different levels of theory for the TS search find asymmetric side-centered TS's with similar geometries. Besides our-

TABLE II. Geometries obtained for the asymmetric side-centered TS of the preparing mechanism. The asterisk means not available.

	$R(\text{H1-H2})/\text{\AA}$	$R(\text{Si1-H1})/\text{\AA}$	$R(\text{Si1-H2})/\text{\AA}$	$R(\text{Si2-H2})/\text{\AA}$	$R(\text{Si1-Si2})/\text{\AA}$	Si1 buckled down?	Level of theory in TS search
This work	0.97	1.71	1.79	2.09	2.52	yes	CSSCF cluster
Jing and Whitten (Ref. 17)	1.02	1.65	1.63	2.11	2.48	yes	CASSCF cluster
Nachtigall, Jordan, and Sosa, (Ref. 18)	0.92	1.75	1.73	2.34	2.41	yes	LDA-DFT slab
Kratzer, Hammer, and Nørskov (Ref. 20)	1.01	1.69	1.78	*	*	yes	LDA-DFT slab
Vittadini and Selloni (Ref. 22)	1.08	1.70	1.79	2.14	*	yes	LDA-DFT slab
Pai and Doren (Ref. 23)	0.99	1.69	1.68	2.18	*	yes	LDA-DFT cluster
disilane 1,2-elimination TS, this work	0.99	1.72	1.78	2.00	2.45		CASSCF

selves, only Kratzer, Hammer, and Nørskov²⁰ have verified that the asymmetric side-centered TS they found is indeed a true TS allowing one-step desorption from the monohydride. Although the TS geometries obtained are similar, the activation energies for the TS vary dramatically (refer to Sec. II). This makes sense, since it is known empirically that lower-level calculations such as HFSCF do well at finding TS geometries (except symmetric TS's, as mentioned earlier), but not at calculating energy differences. Note also that the similarity of the TS geometries obtained by the DFT slab calculations, DFT cluster calculations, and CASSCF cluster calculations again indicates that the cluster model is able to represent the important surface interactions. Finally, the geometry of the asymmetric dimer-centered TS is given in Fig. 3(c). This TS has an activation energy of 3.57 eV, and we have determined that it is also a saddle point of rank 1.

The largest discrepancy in predictions for the structure of the Si surface obtained via DFT and CASSCF methods is that the DFT calculations predict that the bare surface dimer is buckled, while CASSCF methods find that an unbuckled dimer is the minimum-energy configuration. Since the cluster calculation of Pai and Doren²³ shows the same kind of buckling for the bare Si surface that the slab calculations do, we conclude that *surface dimer buckling in the DFT calculations is not due to surface strain* (which has been invoked to explain buckling in an extended surface via interactions between neighboring dimers),⁵¹ *since the cluster has no such strain*. We suspect, instead, that the surface dimer buckling is an artifact of a lack of full electronic correlation in the wave function, since the complete absence of electronic correlation also causes buckling in the ground state of surface Si dimers.³⁵ When electron correlation is explicitly included in a CI expansion, such as in a generalized valence bond^{19,35} (GVB) or CASSCF (see Ref. 17 and this work) wave function the buckling disappears,^{17,19,35} suggesting that the buckled minimum is an artifact of the DFT calculations. While low-temperature STM data suggest the existence of buckled dimers at 120 K,⁵² the very presence of the STM and its associated high electric fields may perturb the electronic ground state of the dimer so much as to make the buckled, charge-polarized dimer the preferred state.⁵³ Thus, the STM data are not unequivocal, and this suggests that deficiencies in the theoretical models of Si surfaces come not from cluster truncation, but perhaps from the use of approximate density functionals.

Given the localized electronic structure expected for a covalently bound solid, one can easily rationalize the high bar-

riers (3.55–3.68 eV) that we find for the preparing mechanism on the basis of the molecular Woodward-Hoffman rules,⁵⁴ which predict that any four-electron process such as this is “forbidden” (i.e., a high barrier for a symmetric approach is predicted). Symmetry breaking, in the case of the two asymmetric barriers, gives equally large activation energies. Presumably this is because the preparing TS's necessitate four-centered, delocalizing bonding over a long (2.44 Å) dimer bond, producing TS's much higher in energy relative to the monohydride. Thus, it is not surprising that the activation energies for all three preparing TS's are substantially higher than experimentally determined values (1.95–2.86 eV).^{2–6} Adsorption barriers for these pathways, however, are consistent with the low sticking probability of H₂ on Si(100), suggesting that desorption may require a different pathway than adsorption. Judging from the high activation barrier we obtain for the preparing mechanism, we might immediately exclude this as the observed pathway for H₂ desorption. However, as the experiments directly measure rate constants, not barriers, we calculated the rate constants for H₂ desorption via the preparing mechanism at the peak temperature of 800 K.

In Table III we summarize the activation energies, preexponentials, and rate constants for H₂ desorption via the three preparing mechanism TS's. The largest calculated rate constant is at least six orders of magnitude lower than the lowest experimentally determined rate constant (0.048–2.77 s⁻¹).^{2–6} Thus the preparing mechanism is determined to be inconsistent with experimental results by our calculated activation energy and rate constant, as well as from the independent calculations of Jing and Whitten¹⁷ and Nachtigall, Jordan, and Sosa.¹⁸ Therefore, we believe that we can unequivocally rule out this mechanism.

The high barrier for the preparing mechanism is analogous to the large activation energy calculated for the 1,2 elimination of H₂ from disilane (~3.7 eV; see Table I). In fact, the TS geometry calculated by us (see Table II) and others for this reaction⁵⁵ looks very similar to the asymmetric side-centered TS's found for the preparing mechanism, including those calculated using slab models. This similarity between the surface TS for H₂ desorption and the gas-phase reaction TS for 1,2 elimination indicates, yet again, that H₂ desorption is a very localized reaction—an ideal reaction for using the cluster approximation to the surface. Instead, H₂ elimination from disilane occurs through the 1,1-elimination pathway, which has an experimentally determined barrier of 2.4 eV.^{56,46} The most similar process on Si(100)–2×1 is H₂ elimination from a dihydride species. One way to create this

TABLE III. Calculated H_2 adsorption and desorption activation energies and rate constants are given for all pathways.

Geometry	E_a desorption (eV)	E_a adsorption (eV)	preexponential desorption (s^{-1})	k desorption 800 K (s^{-1})
$Si_9\bar{H}_{12}H_2$ cluster ($\Theta_H=1$ ML)				
symmetric preparing TS	3.71 (3.55 with zpe)	0.62 (0.65 with zpe)	9.3×10^{14}	4.2×10^{-8}
asymmetric preparing TS (dimer centered)	3.72 (3.57 with zpe)	0.64 (0.67 with zpe)	1.2×10^{15}	4.0×10^{-8}
asymmetric preparing TS (side centered)	3.78 (3.68 with zpe)	0.70 (0.78 with zpe)	1.4×10^{14}	8.7×10^{-10}
dihydride isomerization TS	1.85 (1.80 with zpe)	0.67 (0.65 with zpe)	5.2×10^{15} ^a	3.3×10^{-8} ^a
dihydride isomer to desorbed TS	2.64 (2.94 with zpe)	0.74 (0.78 with zpe)		
$Si_9\bar{H}_{12}H_4$ cluster ($\Theta_H=2$ ML)				
1,2 elimination TS	3.23 (3.08 with zpe)	2.43 (2.47 with zpe)	1.5×10^{15}	7.0×10^{-6}
$Si_{10}\bar{H}_{14}H_2$ cluster				
symmetric TS	4.53 (4.40 with zpe)	2.27 (2.33 with zpe)	6.3×10^{14}	1.1×10^{-13}
asymmetric TS	2.59 (2.49 with zpe)	0.33 (0.42 with zpe)	5.0×10^{12}	9.9×10^{-4}
experimental values	1.91–2.86 ^b		2.2×10^{11} – 6.5×10^{17} ^b	4.8×10^{-2} – 2.77^b

^aCombined rate constant from a two-step process (see Sec. VI B).

^bSee Refs. 2, 3, 4, 5, and 6.

species is through monohydride-dihydride isomerization, and it is this process which we investigate next.

B. Monohydride–dihydride isomerization mechanism

Figure 4 shows the pathway followed by the monohydride-dihydride isomerization mechanism. As noted above, Wu, Ionova, and Carter¹⁹ determined the overall barrier for this reaction to be 4.1 eV by determining activation energies (without zpe corrections) for the monohydride-dihydride isomerization (step 1, $E_a=2.0$ eV), dihydride to monohydride reversion (step -1 , $E_a=0.1$ eV), and desorption from the dihydride (step 2, $E_a=2.2$ eV). In comparison, using a higher level of theory we determine activation barriers (all of which include zpe corrections) of 1.80, 0.65, and 2.53 eV for steps 1, -1 , and 2, respectively. Our calculation leads us to an overall barrier of 3.68 eV ($E_{\text{overall}}=E_{\text{step1}}-E_{\text{step-1}}+E_{\text{step2}}$). The main difference between our calculation and that of Wu, Ionova, and Carter is that we find that the dihydride isomer is more stable relative to the monohydride than do Wu, Ionova, and Carter, leading to our predic-

tion of a larger barrier for dihydride to monohydride reversion and also for desorption from the dihydride. We optimized the geometry of the dihydride isomer [Fig. 5(a)] by fixing the component along the Si-Si “dimer” distance at 3.84 Å (the two surface Si atoms were still allowed to move in the surface normal direction), so that the undimerized Si atoms would not move too far apart, since there are no neighboring Si atoms in our model to prevent this. On a real surface, the Si-Si “dimer” distance would be constrained to be 3.84 Å due to neighboring Si atoms. In contrast, Wu, Ionova, and Carter optimized their structure with no constraints, giving a Si-Si distance of 4.198 Å. Because of the additional constraint placed on our system, it seems that our dihydride isomer should be higher in energy than the structure obtained in Ref. 19. In fact, we find that optimizing the dihydride isomer at the CASSCF level without the constraint on the Si-Si distance lowers the energy of this structure by only a small amount (<0.1 eV). Thus the difference between our calculated values and those in Ref. 19 is not due to this constraint, but instead must be the result of the different levels of theory used; CASSCF/MRSDCI on relatively large

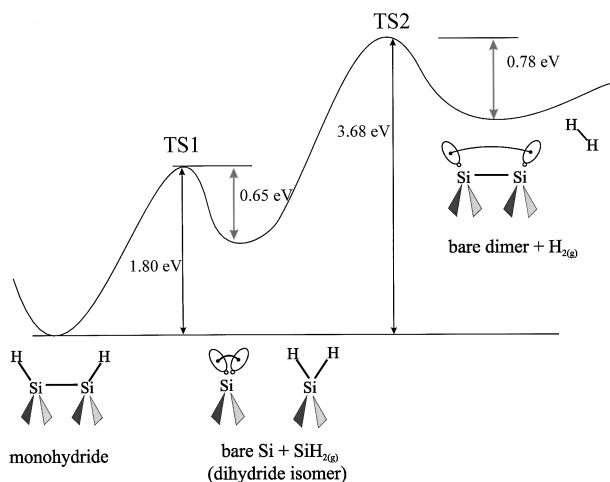


FIG. 4. The reaction pathway and energy barriers for the isomerization mechanism for H_2 desorption.

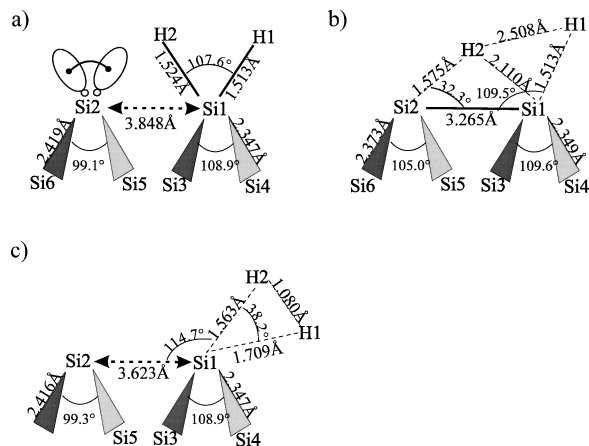
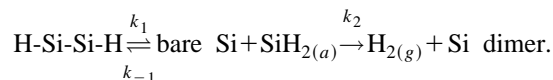


FIG. 5. The geometries for (a) the dihydride isomer, (b) TS1, the TS for dihydride isomerization; and (c) TS2, the TS for desorption from the dihydride isomer (see Fig. 4).

clusters in this work versus GVB/MRSDCI on much smaller clusters in Ref. 19; inclusion (this work) or not (Ref. 19) of zpe corrections; and use (this work) or not (Ref. 19) of bulk-fitted embedding \bar{H} 's.

Note that the activation barriers determined by us (2.5 eV) and by Wu, Ionova, and Carter (2.2 eV) for step 2 (H_2 elimination from a dihydride species), are similar to the activation barriers for 1,1 elimination of H_2 from disilane (2.4 eV) (Refs. 56 and 46) and for H_2 elimination from silane (2.4 eV).⁴⁶ Figures 5(b) and 5(c) show TS geometries for steps 1 and 2, respectively. As we might expect, the geometry for the TS for step 2 [$R(H1-H2)=1.080$ Å, $R(Si1-H1)=1.709$ Å, $R(Si1-H2)=1.563$ Å, $R(Si2-H2)=4.5061$ Å, $R(Si1-Si2)=3.623$ Å, and $\theta(H2-Si1-H2)=38.2^\circ$] shows a TS that is closely related to the TS for silane decomposition determined by us and others.⁵⁷ [We find this gas-phase TS geometry to be $R(H1-H2)=1.148$ Å, $R(Si1-H1)=1.736$ Å, $R(Si1-H2)=1.548$ Å, and $\theta(H2-Si1-H2)=40.4^\circ$, where H1 and H2 label the incipient H_2 molecule]. In fact, from the long Si2-H2 distance, we see that this TS does not involve the neighboring bare Si. In contrast, Wu, Ionova, and Carter's TS [$R(H1-H2)=1.075$ Å, $R(Si1-H1)=1.627$ Å, $R(Si1-H2)=1.618$ Å, $R(Si2-H2)=2.114$ Å, $R(Si1-Si2)=2.538$ Å, and $\theta(H2-Si1-H2)=56.0^\circ$] with a much shorter Si2-H2 distance is surprisingly close in geometry to the asymmetric side-centered TS's given in Table II, most likely because of the lower level of theory (HFSCF) used in the TS search.

We noticed, as did Wu, Ionova, and Carter¹⁹ that the activation energy for desorption from the dihydride isomer is within the range of experimental values for H_2 desorption from Si(100)-2 \times 1, but that the isomerization step boosts the activation barrier for this process well above this range. By setting up a simple kinetic equation for the isomerization mechanism, we can easily determine the effect of the isomerization step on the overall rate constant for this mechanism:



At 800 K, where H_2 desorption is at its peak, we predict $k_1=4.8 \times 10^1$ s⁻¹, $k_1=2.0 \times 10^7$ s⁻¹, and $k_2=1.4 \times 10^{-2}$ s⁻¹. Thus desorption from $SiH_{2(a)}$ is the rate-determining step, and the rate of the reaction is $r=k_2[SiH_{2(a)}]$, where $[SiH_{2(a)}]$ is the coverage of $SiH_{2(a)}$. Since $k_1, k_{-1} \gg k_2$, the equilibrium between the monohydride dimer (H-Si-Si-H) and the dihydride isomer (bare Si + $SiH_{2(a)}$) is reached rapidly, giving $[SiH_{2(a)}]=(k_1/k_{-1})[H-Si-Si-H]$. After substitution, the overall rate becomes $r=(k_1 k_2/k_{-1})[H-Si-Si-H]$ and the overall rate constant is 3.3×10^{-8} s⁻¹. Since 3.3×10^{-8} s⁻¹ \ll 0.048–2.77 s⁻¹, the range of experimentally determined rate constants, there is no ambiguity in ruling out this mechanism for desorption. This leads us to consider the only remaining mechanism: desorption from an isolated dihydride.

C. Desorption from isolated dihydrides

In Fig. 6 we show the energetics for two possible pathways for desorption via an isolated dihydride, for which the endothermicity is predicted to be 2.07 eV (including zpe corrections). Figure 6 also depicts the geometries obtained for

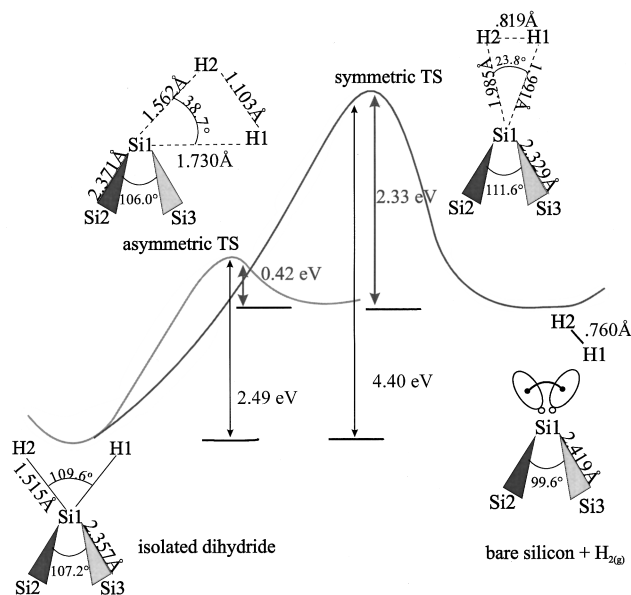


FIG. 6. Two pathways (involving a symmetric or an asymmetric TS) for adsorption/desorption via an isolated dihydride are depicted, along with the geometries of the products, reactant, and respective TS's. It is apparent from the geometries that the TS with the highest-energy barriers for adsorption and desorption (the symmetric TS) is a "late" TS to desorption, and consequently an "early" TS to adsorption, while the asymmetric TS, which has lower-energy barriers for adsorption and desorption, is an "early" TS for desorption and a "late" TS for adsorption. See text for further details.

the symmetric and asymmetric TS's using the $Si_{10}\bar{H}_{14}H_2$ cluster. As with all of the TS's we find, we have verified both TS's to be saddle points of rank 1.⁵⁸

For the symmetric TS, the barrier to desorption is 4.40 eV, much higher than the experimentally observed value for desorption. As we mentioned for the symmetric preparing TS, this high barrier is not unreasonable considering that a symmetric TS is forbidden by the Woodward-Hoffman rules for a four-electron process. Furthermore, the rate constant for desorption at 800 K is 1.1×10^{-13} s⁻¹, which is over ten orders of magnitude lower than the experimentally determined rate constant.

For the asymmetric TS, the barrier to desorption is 2.49 eV (including zpe corrections). This activation energy agrees well with experimental results which span from 1.95–2.86 eV, and is in particularly good agreement with the results of Höfer, Li, and Heinz⁵ ($E_a=2.48 \pm 0.1$ eV), Wise *et al.*³ ($E_a=2.51$ eV), and Flowers *et al.*⁶ ($E_a=2.47$ eV).

Our calculation of the rate constant yields 9.9×10^{-4} s⁻¹, which is lower than the smallest experimentally determined rate constant (0.048–2.77 s⁻¹) by more than one order of magnitude. However, our calculated value for the rate constant is not so low as to exclude this mechanism, unlike the rate constants we obtained for the other mechanisms, which are at least six orders of magnitude too small and thus can be ruled out unambiguously. There are two possibilities for error in our rate constant. The first is that the activation energy we have calculated is too high. Although it is a reasonable approximation to use the $Si_{10}\bar{H}_{14}H_2$ cluster with only one surface Si, since in the monohydride phase other H atoms

would be at least 2.77 \AA away, a defect SiH_2 could feel some lateral repulsion from neighboring monohydrides or even other dihydrides, if present, which might reduce the barrier height. More importantly, from our gas-phase calculations of H_2 elimination from silane we found that our method may overestimate this desorption activation barrier by as much as 0.2 eV . Because the activation energy appears in the exponential in the rate constant expression, even a small reduction in the barrier, such as 0.2 eV would increase the rate constant to 0.02 s^{-1} , nearly within the range of experimental values. Note that even in the most pessimistic case, assuming a 0.4-eV error and subsequent 0.4-eV reduction in the barrier height, the rate constants we have determined for the other mechanisms would still be too low by at least three orders of magnitude. Thus our conclusion to exclude those mechanisms remains unchanged. On the other hand, a 0.4-eV lowering of the barrier in the dihydride pathway would yield a rate constant of 0.3 s^{-1} , in excellent agreement with the experimental values.

The second possible source of error is the preexponential. This could be due to the approximations involved in estimating the rate constant using STST and calculating vibrational frequencies using a numerical rather than analytical Hessian. Although our calculated prefactor of $5.0 \times 10^{12} \text{ s}^{-1}$ is not outside of the experimental range of values ($2.2 \times 10^{11} - 6.5 \times 10^{17} \text{ s}^{-1}$),²⁻⁶ if we compare our results to those results of Refs. 5 ($A \sim 2 \times 10^{15} \text{ s}^{-1}$), 3 ($A \sim 5.5 \times 10^{15} \text{ s}^{-1}$) and 6 ($A \sim 2 \times 10^{15} \text{ s}^{-1}$) we find that our preexponential is three orders of magnitude smaller. If it is the case that we have underestimated the prefactor by this amount, then our rate constant would be $\sim 1.0 \text{ s}^{-1}$, agreeing with the highest rate constants measured. Nonetheless, it is important to point out that even this high degree of error in the preexponential would not make the rate constants of pathways through the other TS's competitive. Of course, it could also be that our rate constant is too low due to a smaller amount of error in both the activation energy and the preexponential. Thus small errors in one or both of our Arrhenius parameters can easily account for the 1–2 order-of-magnitude discrepancy between our calculated rate constant for H_2 desorption from $\text{SiH}_{2(a)}$, and the measured rate constants, but could not bring the rate constants from other proposed mechanisms into agreement with experiment. Therefore, we propose (again) that there is still only one viable candidate for the desorption precursor, namely, $\text{SiH}_{2(a)}$.

In order for us to associate the observed rate constant with desorption from $\text{SiH}_{2(a)}$, it must be that the H_2 desorption step is rate limiting. In order for this to be so, we must suggest how $\text{SiH}_{2(a)}$ may form, and ensure that such formation involves only steps which are fast compared to H_2 desorption. One possible mechanism for creation of $\text{SiH}_{2(a)}$ was recently proposed by Nachtigall, Jordan, and Sosa,¹⁸ and involves the generation of $\text{SiH}_{2(a)}$ from a monohydride species located next to an isolated atom defect site which is perpendicular to the dimer row. The isolated atom defect would react with the monohydride to form a Si dimer and $\text{SiH}_{2(a)}$, with a barrier predicted by DFT (at the Becke3LYP level) to be 1.65 eV . Thus, based on barrier heights, this isomerization is expected to be fast compared to desorption, as we require. Jing, Lucovsky, and Whitten have proposed type- S_B steps as a source of isolated Si atoms³¹ [Figs. 7(a)

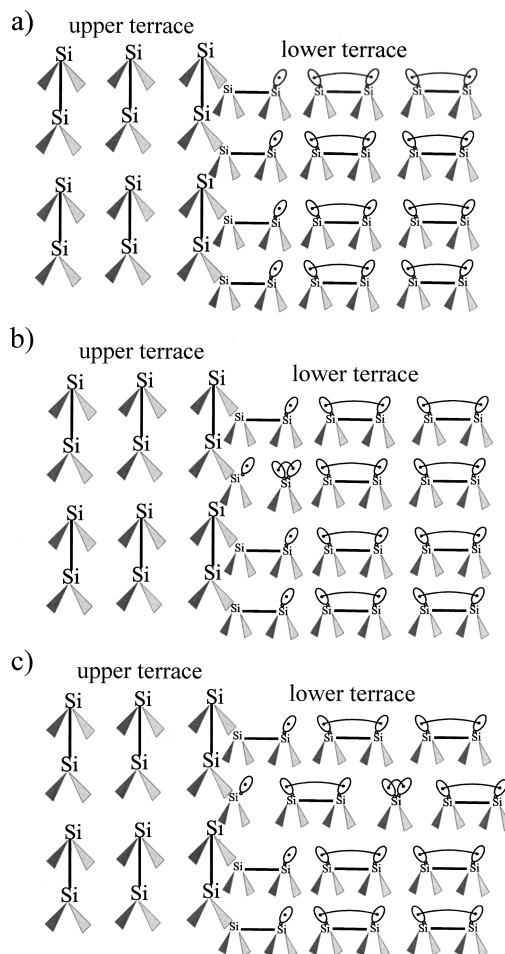


FIG. 7. A type- S_B step. The large or small Si atoms represent surface Si dimer atoms on the upper or lower terrace. (The weakly paired dangling bonds are not shown for upper terrace dimers for viewing clarity.) The step edge is parallel to dimer rows on the lower terrace, and perpendicular to those on the upper terrace. (a) A perfect type- S_B step. Notice that the surface dimer Si atom on the lower terrace closest the step edge is bonded to a surface Si dimer atom on the upper terrace, breaking the weak pairing of the dangling bonds for lower terrace. (b) An isolated Si atom is formed at the step edge. (c) The isolated Si atom migrates away from the step edge.

and 7(b)]. Similarly, defects could be generated at $S_{B'}$ -type steps [Figs. 8(a) and 8(b)]. Once formed, the lone Si atom could migrate away from the step edge [Figs. 7(c) and 8(c)] via a mechanism such as that proposed in Ref. 18 for defect diffusion.¹⁸ The barrier for such defect migration was found to be only 0.61 eV (DFT at the Becke3LYP level), and thus this process also should be fast compared to H_2 desorption, as required.

Both of the mechanisms discussed above require the creation of isolated atom defects. It is true that STM studies⁵⁹ have shown that dimer vacancies are the primary type of defects on Si(100) at room temperature. However, since STM experiments have not been carried out near the H_2 desorption temperature, it is not possible to rule out the presence of isolated atom defects on Si(100) at 800 K . Furthermore, these defect-based mechanisms only require small concentrations of such defects, since they will be catalytically regenerated through H_2 desorption. Thus, if even small

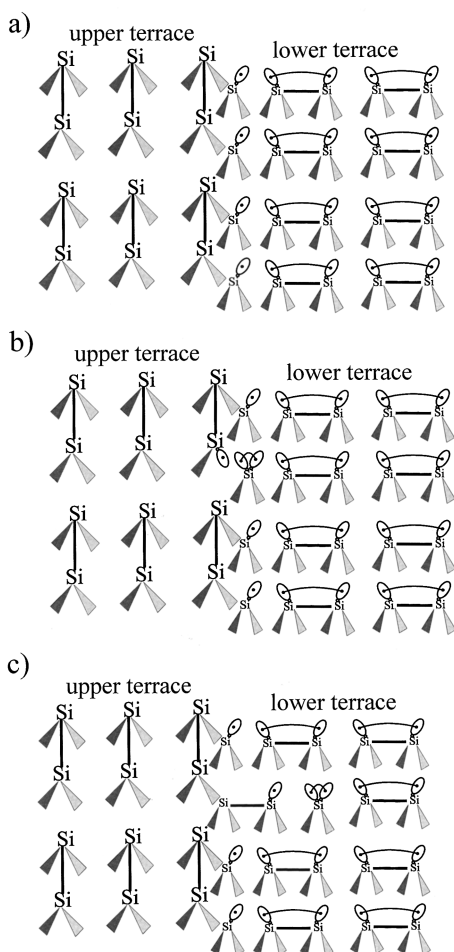


FIG. 8. A type- $S_{B'}$ step. The large or small Si atoms represent surface Si dimer atoms on the upper or lower terrace. (The weakly paired dangling bonds are not shown for upper terrace dimers for viewing clarity.) The step edge is parallel to dimer rows on the lower terrace and perpendicular to those on the upper terrace. (a) A perfect type- $S_{B'}$ step. Notice that atoms on the lower terrace at the step edge have only three bonds, two subsurface bonds, and one bond to a surface Si dimer atom on the upper terrace. (b) An isolated Si atom is formed at the step edge. (c) The isolated Si atom migrates away from the step edge.

concentrations of isolated Si atoms exist at 800 K, this will be sufficient to convert the monohydrides to dihydrides in steps fast relative to H_2 desorption, as required.

Given a rate-limiting step for desorption that involves $SiH_{2(a)}$, it is important to ensure that the coverage of $SiH_{2(a)}$ can be approximately equal to the coverage of H atoms; otherwise, the observed first-order dependence on H-atom coverage cannot be explained by this mechanism. From the discussion directly above, we can now see that $\Theta(SiH_{2(a)}) \sim \Theta(H)$, by noting first that quantitative conversion of the monohydrides ($H-Si-Si-H_{(a)}$) to dihydrides ($SiH_{2(a)}$) by the catalytic action of a small number of isolated Si-atom defects implies that $\Theta(SiH_{2(a)}) \sim \Theta(H-Si-Si-H_{(a)})$. Second, since D'Evelyn and co-workers^{14,16} have previously shown that $\Theta(H-Si-Si-H_{(a)}) \sim \Theta(H)$, then it follows that $\Theta(SiH_{2(a)}) \sim \Theta(H)$.

In summary, we find that the isolated dihydride mechanism is the only mechanism consistent with all experimental kinetic measurements, with respect to barriers, rate constant, and kinetic order.

D. Dynamics of adsorption/desorption via the isolated dihydride model

The dynamics predicted by desorption via the asymmetric isolated dihydride TS are apparent from its geometry (see Fig. 6). Looking at the geometry obtained for the asymmetric TS from the $Si_{10}H_{14}$ cluster [$R(H1-H2)=1.103$ Å, $R(Si-H1)=1.562$ Å, $R(Si-H2)=1.730$ Å, and $\theta(H1-Si-H2)=38.7^\circ$], notice the short Si-H bond lengths and long H-H bond length compared to our calculated CASSCF H_2 bond length of 0.76 Å and surface Si-H bond length of 1.515 Å. Because the TS resembles the initial, adsorbed state, it is termed an ‘‘early’’ TS for desorption. Just as the asymmetric side-centered TS is geometrically close to the analogous disilane reaction, we see that the asymmetric isolated dihydride TS resembles the TS we determined for H_2 elimination from SiH_4 [$R(H1-H2)=1.148$ Å, $R(Si1-H1)=1.548$ Å, $R(Si1-H2)=1.736$ Å, and $\theta(H2-Si1-H2)=40.4^\circ$, where H1 and H2 label the incipient H_2 molecule]. We also find that this isolated dihydride TS is approximated well by previous HFSCF calculations of the TS by Wu, Ionova, and Carter¹⁹ which modeled desorption from an isolated dihydride as the elimination of H_2 from SiH_2H_2 where the geometry of the Si and two H’s were fixed so as to mimic the constraints of the surface. The geometry they obtained for the TS is $R(H1-H2)=1.224$ Å, $R(Si-H1)=1.521$ Å, $R(Si-H2)=1.629$ Å, $\theta(H1-Si-H2)=38.7^\circ$. As Wu, Ionova, and Carter¹⁹ observed in regards to their structure, we also note that the long H-H bond of the asymmetric TS is consistent with the REMPI measurements of Shane, Kolasinski, and Zare,^{12,13} who observed that H_2 desorbing from $Si(100)-2 \times 1$ is vibrationally excited. Furthermore, although Shane, Kolasinski, and Zare determined that desorbing H_2 is rotationally cold compared to a surface temperature of 800 K, they found rotational distributions characteristic of ~ 400 K, which could still be consistent with an asymmetric TS. Indeed, further support for the asymmetric TS is evident in *ab initio* molecular-dynamics (AIMD) simulations⁶⁰ to be reported elsewhere, which suggest a mechanism for possible rotational cooling of H_2 .

As mentioned above, the short Si-H bonds and long H-H bond of the asymmetric TS also indicate that it is an ‘‘early’’ desorption TS. The symmetric TS, on the other hand, has a comparatively short H-H bond (0.819 Å) and long Si-H bonds (~ 2.0 Å), representing a structure closer to the desorbed species and making it a ‘‘late’’ TS for desorption. Thus it is possible that the adsorbed H atoms would see the ‘‘early’’ TS and desorb asymmetrically, while adsorbing H_2 molecules might primarily see the symmetric TS, which is the ‘‘early’’ TS if starting from H_2 gas. We find that the barrier to adsorption is 0.42 eV through the asymmetric pathway, compared to a barrier of 2.33 eV for the symmetric pathway. This raises an interesting suggestion regarding the extremely low sticking probability of H_2 on the $Si(100)-2 \times 1$ surface. If H_2 adsorbs through the same pathway it desorbs through, namely, the asymmetric pathway, then one would expect a higher sticking probability, since the barrier to adsorption would be 0.42 eV (or even much lower due to our

estimation of an ~ 0.2 – 0.5 -eV error for this barrier). However, looking at the geometry of the asymmetric TS, we can see that it involves a bend of the surface SiH_2 sideways, so that one of the H atoms comes to the level of the Si surface. While this type of sideways bend may be possible for the adsorbed H atoms, it would be unlikely for an incoming H_2 molecule to come in at this angle to the surface. Instead the H_2 most probably sees the higher symmetric barrier of 2.33 eV or the high barriers for adsorption onto a Si dimer (~ 0.6 – 0.8 eV) and bounces off unreactively. On the other hand, desorption would occur through the asymmetric TS. The 0.43-eV adsorption barrier we find for this process is higher than the ~ 0.1 -eV barrier observed by Kolasinski *et al.*^{28,29} in H_2 desorption experiments. As noted above, it is possible that we are overestimating this barrier by ~ 0.2 – 0.5 eV. Thus, error estimates alone suggest that the adsorption barrier via the asymmetric isolated dihydride TS is as low 0–0.2 eV, making desorption via this TS consistent with the low adsorption barrier observed by Kolasinski *et al.*^{28,29} It could also be that desorption through the asymmetric isolated dihydride TS involves some energy transfer to surface Si phonons, and this could also contribute to the low measured H_2 translational energies that appear to correspond to a lower barrier.³²

AIMD simulations are also able to explain how H_2 desorbing from the asymmetric TS can be reconciled with angular distribution measurements,⁶¹ which show that D_2 molecules thermally desorbing from $\text{Si}(100)\text{-}2\times 1$ have an angular distribution that is peaked around the surface normal direction (fit to $\cos^{4-5}\theta$). Certainly, examination of the static structure of the asymmetric TS suggests broader angular distributions than those experimentally observed. We have shown with AIMD simulations how desorbing H_2 molecules can become focused in the surface normal direction through surface corrugation effects, and thus can give angular distributions conforming with experimental observations.⁶⁰

It has been observed that the H_2 adsorption probability increases with surface temperature.^{26,28,29,34} Since higher surface temperatures are expected to increase the number of isolated Si species available through Si adatom diffusion,^{62,63} and lone Si atom creation via activated processes, the isolated dihydride mechanism is compatible with these experiments. In fact, we think that the disparity between experimentalists as to the extent of this effect^{26,28,29} can be explained by different concentrations of isolated Si atom defects on the surface. Indeed, a related explanation for the increase in sticking probability with higher surface temperatures has been given by Kolasinski *et al.*^{28,29} who proposed that lone Si atoms are created transiently due to thermal disorder. As the temperature rises, so does the amount of disorder, leading to more adsorption sites, and thus increasing the H_2 adsorption probability.

It is important to emphasize that a mechanism explaining the apparent violation of detailed balance involving multiple pathways is not in violation of the second law of thermodynamics. This is because experiments of the adsorption/desorption of H_2 on $\text{Si}(100)$ are not performed at equilibrium, and thus the second law of thermodynamics does not apply. Our calculations coincide with the nonequilibrium conditions of the experiments, since we attempt to find all available kinetic pathways for adsorption/desorption. Indeed,

when incoming H_2 molecules do find the correct orientation to adsorb, adsorption presumably happens through the lowest energy pathway (the asymmetric TS), the pathway through which desorption also occurs. To our knowledge no experiments have been done to determine the effect of the H_2 beam incident angle on the sticking probability. The fact that the lowest adsorption barrier we find is the orientationally constrained asymmetric TS suggests that impinging H_2 molecules directed at the surface at a grazing angle might have a higher probability for adsorption than H_2 directed normal to the surface. Furthermore, since the asymmetric TS is a “late” TS to adsorption, with a H-H distance 45% longer than the equilibrium bond distance for free H_2 , we suggest that vibrational excitation of the impinging H_2 molecule should also enhance adsorption.

E. Desorption from the $\text{Si}(100)$ dihydride phase ($\Theta_{\text{H}}=2.0$ ML)

Since the REMPI measurements of Shane, Kolasinski, and Zare^{12,13} indicate that H_2 desorbs from the $\text{Si}(100)$ dihydride phase through the same precursor as it does from the $\text{Si}(100)$ monohydride phase, we suggest (as did Wu, Ionova, and Carter¹⁹ previously) that desorption from the dihydride surface also occurs through the $\text{SiH}_{2(a)}$ species. Our calculated barrier for desorption from $\text{SiH}_{2(a)}$ (2.49 eV) agrees well with the most accurate experimental measurements (2.48 ± 0.1 – 2.51 ± 0.1 eV) (Refs. 3, 5, and 6) of H_2 desorption from the monohydride phase. However, it is significantly higher than the experimentally determined barrier for desorption from the dihydride phase (1.9–2.0 eV).^{6,64} A reduction in barrier height for desorption from the dihydride phase could be due to lateral interactions with other dihydrides or surface species with $\text{SiH}_{2(a)}$. The repulsions of neighboring species could destabilize $\text{SiH}_{2(a)}$ more than the TS and thus lower the barrier to desorption. Even with the improvement in modern computing power, we are unable to model a surface as complicated as the dihydride surface, a surface which also may be comprised of monohydrides and trihydrides,⁶⁵ at an adequate level of theory to test this hypothesis. However, we are able to determine the activation energy for possibly the only other alternative to desorption on the dihydride surface, 1,2 desorption from neighboring dihydrides leaving behind a monohydride [$\text{SiH}_{2(a)} + \text{SiH}_{2(a)} \rightarrow \text{H-Si-Si-H}_{(a)} + \text{H}_{2(g)}$]. This mechanism was proposed by Ciraci and Batra⁶⁶ who used LDA-DFT slab calculations with an 8-Ry cutoff to estimate that such a process would have an ~ 1.5 -eV barrier to desorption. On the other hand, using LDA-GGA DFT slab calculations, Vittadini and Selloni²² did a rough TS search and determined that although they calculated that 1,2 desorption is a slightly exothermic process, it would have a much higher activation energy than the activation energy for 1,1 desorption (desorption from a single dihydride species), the latter which they place at ~ 2 eV (not including zpe corrections).

We used an $\text{Si}_9\text{H}_{12}\text{H}_4$ cluster to model 1,2 elimination of H_2 from two neighboring dihydride species to form $\text{H}_{2(g)}$ and a monohydride. Geometries of the optimized dihydride “surface” and the 1,2-elimination TS are given in Figs. 9(a) and 9(b), respectively. The optimal geometry for the dihydride surface was obtained using a constraint of 3.84 Å for the distance between surface Si atoms in the “dimer bond” di-

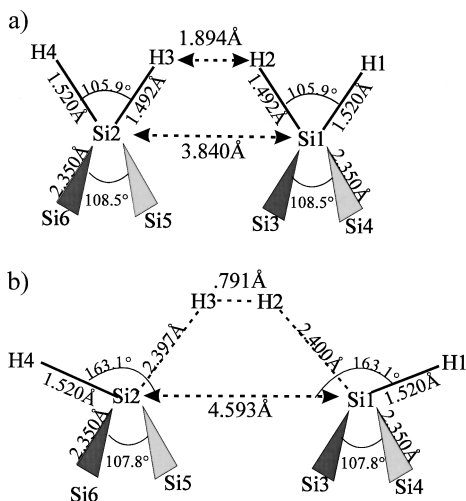


FIG. 9. The geometries obtained for (a) an “ideal” dihydride surface and for (b) the 1,2-elimination TS using an $\text{Si}_9\text{H}_{12}\text{H}_4$ cluster to represent the dihydride surface. During geometry optimization of the ideal dihydride surface (a), the distance between the surface Si’s along the “dimer” bond axis was fixed at the ideal 3.84-Å distance. This constraint was eliminated during the search for the TS (b).

reaction, but the two surface Si atoms were still allowed to move in the surface normal direction. This constraint was used to compensate for the edge effects of the $\text{Si}_9\text{H}_{12}\text{H}_4$ cluster, which make it favorable for the $\text{SiH}_{2(a)}$ units to move apart. The geometry for the monohydride is the same as that shown in Fig. 2. We calculated, including zpe corrections, an endothermicity of 0.61 eV and an activation energy of 3.08 eV for this process. Since the cluster we used consists of only two dihydride species, our calculations did not include the effects of lateral interactions with other surface dihydrides. Lateral repulsions between neighboring hydrides presumably would influence the dihydride species more than the monohydride species, since the monohydride would be farther away from neighboring species. Thus our cluster model probably overestimates the stability of the dihydride phase and thus the endothermicity of this reaction. This overestimation would be the same for both 1,1- and 1,2-elimination processes. The TS for the 1,2 elimination [Fig. 9(b)] would also be less stable in a real system, since it consists of a long Si1-Si2 distance (4.95 Å) and Si-H bonds nearly parallel to the surface, factors which would lead to severe lateral repulsion from neighboring dihydride units. If the lack of repulsive interactions from neighboring dihydrides in our model leads to an equal overstabilization of the dihydride and the 1,2 elimination TS, there is no change in the activation barrier. However, it seems likely that the sprawling structure of the 1,2-elimination TS would experience greater lateral repulsions in a real dihydride phase (recall the huge surface Si-Si distance of 4.59 Å for our ideal TS which would never be allowed on a real dihydride surface where surface Si distances are 3.84 Å) than the dihydride species which is already constrained to the ideal surface geometry (3.84 Å). This suggests that we are underestimating the barrier for 1,2 elimination. Since our calculated barrier is already over 1-eV higher than the experimental results, we do not think that desorption via 1,2 elimination in the dihydride phase is probable.

The 1,1-elimination TS also could be stabilized or destabilized by neighboring species. Theoretical calculations^{66,67} suggest that a “canted” dihydride phase, wherein the dihydride units are tilted away from the ideal tetrahedral geometry, is thermodynamically favored over an ideal dihydride phase, since repulsions between dihydride species are reduced in the canted phase. We propose that since the Si-H bonds are already bent away from their ideal positions (the position they would be in if they were in an isolated dihydride unit) due to dihydride-dihydride repulsions, the energy barrier for desorption from the asymmetric TS should be lowered, since some of the energy required to move the dihydride species from its ideal position to the TS configuration has already been provided—making the asymmetric TS easier to access. On the other hand, the 1,2-elimination pathway would be more difficult to access in a canted phase since in this phase the H atoms on the adjacent dihydride species involved in the TS would be farther away. Furthermore, the 1,2-elimination barrier is likely to be increased in the canted phase, since the TS is destabilized by repulsive interactions with neighbors, while the dihydride canted phase is predicted to be more stable than the perfect tetrahedral dihydride phase. This is unlike the 1,1-elimination TS, which is similar to canted phase dihydrides and thus experiences similarly reduced repulsions, with no net change to the barrier height. Therefore, it seems reasonable to conclude that the 1,2-desorption mechanism is not viable and that our calculated barrier for desorption from an isolated dihydride (2.49 eV) could be lowered significantly at H coverages greater than 1 ML, making the isolated dihydride model consistent with experimental results for the dihydride Si(100) surface. This would result in a common precursor to desorption on the monohydride and dihydride Si(100) surfaces, agreeing with the REMPI results of Shane, Kolasinski, and Zare.

VII. CONCLUSIONS

We have looked at three contending pathways proposed for H_2 desorption from Si(100)- 2×1 and calculated activation energies and rate constants for these mechanisms. We find that the activation energies for all proposed mechanisms other than the isolated dihydride mechanism are at least 0.9 eV higher than the experimentally determined barrier. By contrast, the activation energy for desorption via isolated dihydrides (2.49 eV) is in excellent agreement with the most accurate experimental values.^{3,5,6} We also find that while our estimated rate constant for desorption is somewhat lower than required to explain experimental results, the estimated rate constants of all other mechanisms are at least six orders of magnitude smaller than the range of experimentally determined rate constants. However, small errors in our activation energy (we find our method overestimates H_2 elimination activation energies by ~ 0.1 – 0.2 eV) or approximations inherent to our estimation of the rate constant could bring the rate constant for desorption via isolated dihydrides within the experimental range of values, while these same errors would not be able to account for the six order of magnitude difference between all other mechanisms and experiment.

We also predict that the isolated dihydride mechanism can be compatible with all of the experimental dynamical observations. We propose that the most troublesome of these, the

apparent violation of detailed balance, can be resolved within the framework of this mechanism: desorption occurs through the asymmetric isolated dihydride TS which has a low barrier to adsorption; however, adsorption through this TS is a rare event which can occur only when certain orientational restrictions are overcome and approaching H₂ molecules are more likely to see the higher adsorption barriers of the prepairing TS's or the symmetric isolated dihydride TS and scatter nonreactively. We suggest that H₂ molecules impacting the surface at a grazing angle may have a higher sticking probability, and that increasing the vibrational energy of the impinging H₂ molecules may also lead to enhanced adsorption. The observation of enhanced H₂ adsorption as the surface temperature increases can be understood via the increased concentration of isolated Si atoms with increasing temperature, as required by this mechanism.

The isolated dihydride mechanism has the advantage of being able to explain the REMPI measurements of Shane, Kolasinski, and Zare, which imply a common precursor to desorption from the monohydride and dihydride phases of Si(100) and from Si(111)-7×7. For the Si(100) dihydride phase ($\Theta_{\text{H}}=2$ ML), we suggest that the canted nature of this surface should reduce the barrier required for desorption, explaining the lower activation barrier on the dihydride versus monohydride surfaces. For the Si(111)-7×7 surface, we find that the measured activation energy for H₂ desorption from 2.4±0.1–2.7±0.2 eV (Refs. 3 and 68–70) corresponds well to the calculated value for desorption on Si(111)-2×1 via an isolated dihydride. On the Si(111)-7×7 surface, we expect that the observed second-order dependence on H coverage for desorption is most likely due to relatively fast H diffusion (which has an activation barrier of 1.5±0.2 eV on this surface) (Ref. 71) that precedes the formation of the dihydride precursor. This situation is analogous to H₂ desorption from metal surfaces.

As DFT cluster and slab calculations give similar results in H₂ desorption studies,^{20–24} we conclude that a properly embedded cluster of 9–10 Si atoms models a slab well, and suggest that differences between MRSDCI cluster calculations and DFT calculations are due to CI and DFT approxi-

mations only and not the cluster model. We also question recent DFT calculations^{20–24} which find kinetic support for desorption via the prepairing mechanism, since DFT calculations done with better quality functionals such as the Becke3LYP functional,¹⁸ as well as CASSCF,⁷² MRSDCI (this work), and quadratic configuration interaction with single, double (and perturbative triple) excitations [QCISD(T)] (Ref. 18) calculations all show that the prepairing desorption barrier is at least 0.7 eV higher than the most reliable experimental values (2.4–2.6 eV).^{3,5,6} Furthermore, since it has been shown by others that DFT calculations tend to *underestimate* activation barriers, it would be interesting to know the corresponding value, predicted by the same level of DFT calculations which support the prepairing mechanism, for the barrier to desorption via the isolated dihydride mechanism—we suspect it would be lower than the desorption barrier calculated for the prepairing mechanism at this same level of theory.

In summary, we have provided theoretical evidence that the isolated dihydride mechanism is the only mechanism which is consistent with all experimental observations of kinetics (order, activation energy, and rate constant) and dynamics (violation of detailed balance, internal state and angular distributions, and temperature dependence of sticking probability) of H₂ desorption/adsorption from Si(100)-2×1. Additionally, we have suggested a possible test of this mechanism, namely, grazing-incidence H₂ molecular-beam experiments at high temperatures.

ACKNOWLEDGMENTS

This work was primarily supported by the Air Force Office of Scientific Research. We are grateful to UCLA's Office of Academic Computing staff for help and for providing computer time on the IBM SP2 at UCLA, which is supported by grant funds from the IBM Corporation. E.A.C. also acknowledges the Camille and Henry Dreyfus Foundation and the Alfred P. Sloan Foundation for Teacher-Scholar and Research Fellow Awards, respectively. M.R.R. acknowledges the Gregory Award for Excellence in Research.

* Author to whom correspondence should be addressed.

¹S. F. Shane, K. W. Kolasinski, and R. N. Zare, *J. Chem. Phys.* **97**, 3704 (1992).

²K. Sinniah, M. G. Sherman, L. B. Lewis, W. H. Weinberg, J. T. Yates, Jr., and K. C. Janda, *J. Chem. Phys.* **92**, 5700 (1990).

³M. L. Wise, B. G. Koehler, P. Gupta, P. A. Coon, and S. M. George, *Surf. Sci.* **258**, 5482 (1991).

⁴K. Sinniah, M. G. Sherman, L. B. Lewis, W. H. Weinberg, J. T. Yates, Jr., and K. C. Janda, *Phys. Rev. Lett.* **62**, 567 (1989).

⁵U. Höfer, L. Li, and T. F. Heinz, *Phys. Rev. B* **45**, 9485 (1992).

⁶M. C. Flowers, N. B. H. Jonathan, Y. Liu, and A. Morris, *J. Chem. Phys.* **99**, 7038 (1993).

⁷C. J. Wu and E. A. Carter, *Phys. Rev. B* **46**, 4651 (1992).

⁸A. Vittadini, A. Selloni, and M. Casarin, *Surf. Sci. Lett.* **289**, L625 (1993).

⁹C. J. Wu, I. V. Ionova, and E. A. Carter, *Phys. Rev. B* **49**, 13 488 (1994).

¹⁰P. Nachtigall, K. D. Jordan, and K. C. Janda, *J. Chem. Phys.* **95**, 8652 (1991).

¹¹C. J. Wu and E. A. Carter, *Chem. Phys. Lett.* **185**, 172 (1991).

¹²K. W. Kolasinski, S. F. Shane, and R. N. Zare, *J. Chem. Phys.* **96**, 3995 (1992).

¹³K. W. Kolasinski, S. F. Shane, and R. N. Zare, *J. Chem. Phys.* **95**, 5482 (1991); S. F. Shane, K. W. Kolasinski, and R. N. Zare, *J. Vac. Sci. Technol. A* **10**, 2287 (1992); S. F. Shane, K. W. Kolasinski, and R. N. Zare, *J. Chem. Phys.* **97**, 1520 (1992); **97**, 3704 (1992).

¹⁴M. P. D'Evelyn, Y. L. Yang, and L. F. Sutcu, *J. Chem. Phys.* **96**, 852 (1992).

¹⁵J. J. Boland, *Phys. Rev. Lett.* **67**, 1539 (1991); *J. Vac. Sci. Technol. A* **10**, 2458 (1992).

¹⁶Y. L. Yang and M. P. D'Evelyn, *J. Vac. Sci. Technol. A* **11**, 2200 (1993).

¹⁷Z. Jing and J. L. Whitten, *J. Chem. Phys.* **102**, 3867 (1995).

¹⁸P. Nachtigall, K. D. Jordan, and C. Sosa, *J. Chem. Phys.* **101**, 8073 (1994).

¹⁹C. J. Wu, I. V. Ionova, and E. A. Carter, *Surf. Sci.* **295**, 64 (1993).

- ²⁰P. Kratzer, B. Hammer, and J. K. Nørskov, *Chem. Phys. Lett.* **229**, 645 (1994); P. Kratzer, B. Hammer, and J. K. Nørskov, *Phys. Rev. B* **51**, 13 432 (1995).
- ²¹E. Pehlke and M. Scheffler, *Phys. Rev. Lett.* **74**, 952 (1995).
- ²²A. Vittadini and A. Selloni, *Chem. Phys. Lett.* **235**, 334 (1995).
- ²³S. Pai and D. Doren, *J. Chem. Phys.* **103**, 1232 (1995).
- ²⁴G. Li, Y.-C. Chang, R. Tsu, and J. E. Greene, *Surf. Sci.* **330**, 20 (1995).
- ²⁵P. Nachtigall and K. D. Jordan, *J. Chem. Phys.* **102**, 8249 (1995); P. Nachtigall, K. D. Jordan, A. Smith, and H. Jónsson, *ibid.* **104**, 148 (1996).
- ²⁶P. Bratu, K. L. Kompa, and U. Höfer, *Chem. Phys. Lett.* **251**, 1 (1996).
- ²⁷P. Bratu and U. Höfer, *Phys. Rev. Lett.* **74**, 1625 (1995).
- ²⁸K. W. Kolasinski, W. Nessler, A. de Meijere, and E. Hasselbrink, *Phys. Rev. Lett.* **72**, 1356 (1994); K. W. Kolasinski, W. Nessler, K.-H. Bornscheuer, and E. Hasselbrink, *Surf. Sci.* **331**, 485 (1995).
- ²⁹K. W. Kolasinski, W. Nessler, K.-H. Bornscheuer, and E. Hasselbrink, *J. Chem. Phys.* **101**, 7082 (1994).
- ³⁰S. F. Shane, K. W. Kolasinski and R. N. Zare, *J. Vac. Sci. Technol. A* **10**, 2287 (1992); S. F. Shane, K. W. Kolasinski and R. N. Zare, *J. Chem. Phys.* **97**, 1520 (1992); **96**, 3995 (1992).
- ³¹Z. Jing, G. Lucovsky, and J. L. Whitten, *Surf. Sci. Lett.* **296**, L33 (1993).
- ³²W. Brenig, A. Gross, and R. Russ, *Z. Phys. B* **96**, 231 (1994).
- ³³P. C. Weakliem, G. W. Smith, and E. A. Carter, *Surf. Sci. Lett.* **232**, L219 (1990).
- ³⁴P. Bratu and U. Höfer, *Phys. Rev. Lett.* **74**, 1625 (1995).
- ³⁵A. Redondo and W. A. Goddard III, *J. Vac. Sci. Technol.* **21**, 344 (1982).
- ³⁶C. J. Wu and E. A. Carter, *Phys. Rev. B* **45**, 9065 (1992).
- ³⁷A. K. Rappé, T. A. Smedley, and W. A. Goddard III, *J. Phys. Chem.* **85**, 1662 (1981).
- ³⁸T. H. Dunning, Jr., *J. Chem. Phys.* **53**, 2823 (1970).
- ³⁹S. Huzinaga, *J. Chem. Phys.* **42**, 1293 (1965).
- ⁴⁰R. Fletcher, *Practical Methods of Optimization* (Wiley, New York, 1987).
- ⁴¹I. V. Ionova and E. A. Carter, *J. Chem. Phys.* **98**, 6377 (1993).
- ⁴²I. V. Ionova and E. A. Carter, *J. Chem. Phys.* **103**, 5437 (1995).
- ⁴³M. Dupuis, A. Marquez, and E. R. Davidson, "HONDO 95.3 from CHEM-Station" (IBM, Kingston, NY, 1995).
- ⁴⁴P. E. M. Siegbahn, *J. Chem. Phys.* **74**, 1647 (1980).
- ⁴⁵The total error in our method is found by comparing our CASSCF/MRSDCI calculations of the energetics of these gas-phase systems using basis sets described in Sec. V A, to experimental values (see Table I). In order to understand the origin of our errors, we also estimated the error due solely to our use of ecp's and a finite basis set by comparing these energetics to values obtained using the same level of CASSCF/MRSDCI theory but with a significantly larger basis set [McLean-Chandler basis set for Si including three sets of d functions and a $311++G$ basis set for H with three sets of p functions denoted as MC-311++ $G(3d,3p)$. For basis sets, see A. D. McLean and G. S. Chandler, *J. Chem. Phys.* **72**, 5639 (1980); M. J. Frisch, J. A. Pople, and J. S. Binkley, *ibid.* **80**, 3265 (1984); R. Krishnan, J. S. Binkley, R. Seeger, J. A. Pople, *ibid.* **72**, 650 (1980)]. Based on these calculations, we conclude that the use of ecp's and a smaller basis set leads to a <0.1 -eV overestimation of the energetics. The error implicit in the MRSDCI level of theory then is the total error in our calculations minus the basis set error.
- ⁴⁶H. K. Moffat, K. F. Jensen, and R. W. Carr, *J. Phys. Chem.* **96**, 7695 (1992).
- ⁴⁷J. M. Jasinski and R. D. Estes, IBM Res. Rep. No. 49067.
- ⁴⁸J. M. Jasinski, *J. Phys. Chem.* **90**, 555 (1986).
- ⁴⁹B. Rusic and J. Berkowitz, *J. Chem. Phys.* **95**, 2416 (1991).
- ⁵⁰J. I. Steinfield, J. S. Francisco, and W. L. Hase, *Chemical Kinetics and Dynamics* (Prentice-Hall, Englewood Cliffs, NJ 1989).
- ⁵¹A. Garcia and J. E. Northrup, *Phys. Rev. B* **48**, 17 350 (1993).
- ⁵²R. A. Wolkow, *Phys. Rev. Lett.* **68**, 2636 (1992).
- ⁵³Z. H. Huang, M. Weimer, R. E. Allen, and H. Lim, *J. Vac. Sci. Technol. A* **10**, 974 (1992).
- ⁵⁴R. B. Woodward and R. Hoffman, *The Conservation of Orbital Symmetry* (Verlag-Chemie, Weinheim, 1970).
- ⁵⁵M. S. Gordon, T. N. Truong, and E. K. Bonderson, *J. Am. Chem. Soc.* **108**, 1421 (1986).
- ⁵⁶J. Dzarnoski, S. F. Rickborn, H. E. O'Neal, and M. A. Ring, *Organometallics* **1**, 1217 (1982).
- ⁵⁷M. S. Gordon, D. R. Gano, J. S. Binkley, and M. J. Frisch, *J. Am. Chem. Soc.* **108**, 2191 (1986).
- ⁵⁸A preliminary account of the work in Secs. VI C and VI D is given in M. R. Radeke and E. A. Carter, *Surf. Sci.* **355**, L289 (1996).
- ⁵⁹R. J. Hamers, R. M. Tromp, and J. E. Demuth, *Phys. Rev. B* **34**, 5343 (1986); Ph. Avouris and D. Cahill, *Ultramicroscopy* **42-44**, 838 (1992).
- ⁶⁰A. J. R. da Silva, M. R. Radeke, and E. A. Carter, submitted (1996).
- ⁶¹Y.-S. Park, J.-S. Bang, and J. Lee, *Surf. Sci.* **283**, 209 (1993); *J. Chem. Phys.* **98**, 757 (1993).
- ⁶²Y. W. Mo, J. Kleiner, M. B. Webb, and M. G. Lagally, *Phys. Rev. Lett.* **66**, 1998 (1991); Y. W. Mo, J. Kleiner, M. B. Webb, and M. G. Lagally, *Surf. Sci.* **268**, 275 (1992).
- ⁶³T. Doi, M. Ichikawa, S. Hosoki, and K. Ninomiya, *Surf. Sci.* **343**, 24 (1995).
- ⁶⁴P. Gupta, V. L. Colvin, and S. M. George, *Phys. Rev. B* **37**, 8234 (1988).
- ⁶⁵C. C. Cheng and J. T. Yates, Jr., *Phys. Rev. B* **43**, 4041 (1991); J. J. Boland, *Phys. Rev. Lett.* **65**, 3325 (1990); Y. Wang, M. Shi, and J. W. Rabalais, *Phys. Rev. B* **48**, 1678 (1993).
- ⁶⁶S. Ciraci and I. P. Batra, *Surf. Sci.* **178**, 80 (1986).
- ⁶⁷Preliminary calculations by the authors of a dihydride surface based on the interactions of 6–7 $\text{SiH}_{2(a)}$ units (made of $\text{SiH}_2\bar{\text{H}}_2$ units with the $\bar{\text{H}}$'s fixed in bulk positions) suggest that a canted phase lowers the energy of the dihydride phase by reducing the distance between neighboring H atoms at the cost of moving the Si-H bonds away from their ideal tetrahedral positions.
- ⁶⁸G. A. Reider, U. Höfer, and T. F. Heinz, *J. Chem. Phys.* **94**, 4080 (1991).
- ⁶⁹G. Schulze and M. Henzler, *Surf. Sci.* **124**, 336 (1983).
- ⁷⁰B. G. Koehler, C. H. Mak, D. A. Arthur, P. A. Coon, and S. M. George, *J. Chem. Phys.* **89**, 1709 (1988).
- ⁷¹G. A. Reider, U. Höfer, and T. F. Heinz, *Phys. Rev. Lett.* **66**, 1994 (1991).
- ⁷²Z. Jing and J. L. Whitten, *J. Chem. Phys.* **102**, 3867 (1995).